

CFAR Different Schemes Behavior and Detection Performance of Moving Targets

Ahmed I. Salem¹, Nema M. Elfaramawy², and El-Sayed A. El-Badawy³

¹*Elect. Eng. Dept, Fac. of Eng., Alexandria Univ., Alexandria 21544, Egypt, Student Member IEEE, ahmedsalem@ieee.org*

²*Elect. Eng. Dept, Fac. of Eng., Alexandria Univ., Alexandria 21544, Egypt, n_elfaramawy@yahoo.com*

³*Higher Inst. Of Eng., Thebes Academy, Cairo 11343, and EED, Alex. Univ., Alex. 21544, Egypt SM IEEE, sbadawy@hotmail.com*

Abstract

In this paper detection probability of different CFAR schemes CA, GO, SO, and OS-CFAR is computed via various values of false alarm probability. The CA-CFAR and GO-CFAR detection performance is superior over other schemes; OS-CFAR detection performance appears to be the quasi of CA-CFAR but needs more processing time than CA-CFAR. Moving target detection is investigated. Each of the CA, GO, OS-CFAR schemes gives acceptable detection probability at higher values of SNR and gives, as well, maximum performance in the range of 10^{-4} to 10^{-6} probability of false alarm. The SO-CFAR scheme doesn't offer any advantage over other CFAR processors.

I. INTRODUCTION

Constant False Alarm Rate (CFAR) is a property of threshold that maintains an approximately constant rate of false target detection when the noise in the detector and occasionally in the presence of clutter and ECM (Electronic Counter Measures) are of variable levels. CFAR techniques are used in reception and signal processing to avoid increased false-alarm rates in the presence of jamming, clutter residue, or other interferences [1].

The most basic form of the adaptive threshold processor is the well-known *Cell Averaging* CFAR (CA-CFAR). The input to the processor is the output of the envelope detector, which is sampled in range (and Doppler shifted if possible). Each sample in the range for Doppler shift is named a cell. The test cell is the cell at which a detection decision has to be made [2]. The interference power in each test cell is estimated using its surrounding cells, which are termed reference cells. Under the condition that the sample in each reference cell is independent and identically distributed (*iid*) and with the CA-CFAR algorithm if the assumption of identical statistics of the reference cells is not valid.

In practice there are common situations where such an assumption no longer holds; (i) there is a clutter edge (e.g., at the border of land and sea), where the energy of interference changes, and (ii) there is an outlier, e.g. a clutter spike, an impulsive interference or another interfering target. The resultant CA-CFAR has drawbacks masking weaker targets near stronger targets, excessive false alarms at clutter transitions, and missing of targets near clutter edges.

To accomplish the adaptation in the presence of multiple targets and clutter power transition within the reference window, many modification of the conventional CA-CFAR have been proposed in the

literature [3], [4]. In general these modifications can be classified into two groups depending on whether or not the algorithms rely on ordering of the reference samples for sample selection. The group of CFAR algorithms that do not use rank ordering includes the **S**maller **O**f CFAR (SO-CFAR) which is designed to improve target detection in presence of multiple targets and the **G**reater **O**f CFAR (GO-CFAR) which is designed to minimize the false alarm at clutter edges. The group of CFAR which algorithms that rely on rank ordering includes the **O**rders **S**tatic CFAR (OS-CFAR) [5].

In this paper comparative study of some representatives of the two groups based on Raleigh target and noise models had been investigated and the results reveal that the rank ordering CFAR schemes have better overall performance than those without rank ordering except CA-CFAR which behaves as a quasi OS-CFAR at different values of false alarm probability [6], [7].

The paper is organized as follows. The basic assumptions that have been used to demonstrate the performance of the CFAR processors along with the optimum detector performance are discussed in Section II. Section III reviews of the CA-CFAR processor, and exact expressions for the performance of GO-CFAR, SO-CFAR processor and the OS-CFAR processor for both regions of clutter transitions and multiple target environments. In Section VI simulation results of false alarm rate versus detection probability at various values of SNR are investigated for all CFAR schemes at number of cells ($N=8, 32$) and eventually with conclusions in Section V.

II. BASIC ASSUMPTIONS AND MODEL DESCRIPTION

In a general CFAR detection scheme the square-law detected video range samples are sent serially into a shift register of length $N + 1 = 2n + 1$ as shown in Figure 1(a). The statistic Z which is proportional to the estimate of total noise power is formed by processing the contents of N reference cells surrounding the cell under investigation (or the test cell) whose content is Y . A target is declared to be present if Y exceeds the threshold TZ . Here T is a constant scale factor used to achieve a desired constant false alarm probability for a given window of size N when the total background noise is homogeneous. The processor configuration varies with different CFAR schemes. For example: Figure 1(b) shows the mean level CFAR detection schemes. The processor consists of two summers forming sums Y_1 and Y_2 for the leading and lagging windows. In the CA-CFAR processor Z is simply the sum of Y_1 and Y_2 and in the GO-CFAR and the SO-CFAR processors it is the larger or smaller of the

outputs Y_1 and Y_2 , respectively.

The OS-CFAR processor is shown in Figure 1(c) and involves a sort routine. The k th largest range cell is selected to determine the threshold.

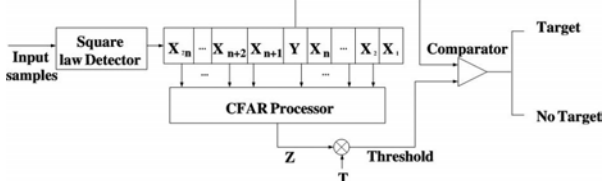


Figure 1. (a) Block diagram of typical CFAR processor

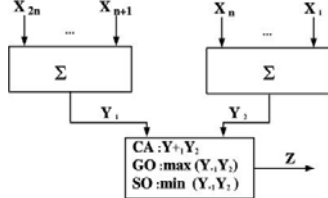


Figure 1. (b) Mean-level CFAR processors.

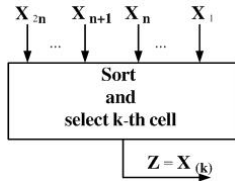


Figure 1. (c) OS-CFAR processor

III. MEAN LEVEL CFAR PROCESSORS DEMONSTRATION

Mean-level CFAR processors incorporate arithmetic averaging to estimate the total noise power. Such detectors are specifically tailored to provide good estimates of the noise power in the exponential pdf. In this section, we describe four such CFAR processors, namely the CA-, GO-, SO- and OS-CFAR processors, for their performance in homogeneous backgrounds as well as in regions of clutter transitions and in multiple target environments, and obtain closed-form performance expressions in each case [4].

A. Cell Averaging CFAR Processor Description

In the CA-CFAR processor, total noise power is estimated by the sum of N range cells of the reference window. This is a complete, sufficient statistic for the noise power under the assumption of exponentially distributed homogeneous noise background. For this processor we have

$$Z = \sum_{i=1}^N X_i \quad (1)$$

where X_i 's are range cells surrounding the cell under test. The exponential density is a special case of the gamma density with $\alpha = 1$ in the pdf

$$f(y) = \beta^{-\alpha} y^{\alpha-1} \exp(-y/\beta) / \Gamma(\alpha), \quad (2)$$

$$y \geq 0, \alpha \geq 0, \beta \geq 0$$

where $\Gamma(\alpha)$ denotes the usual gamma function which has value $(\alpha - 1)!$ for integer α . The cumulative distribution function (cdf) corresponding to this pdf is denoted by $G(\alpha, \beta)$. We write $Y \sim G(\alpha, \beta)$ to mean that Y is a random variable with pdf given in (2). The magnitude of gamma function (mgf) corresponding to the $G(\alpha, \beta)$ distribution is

$$M_Y(u) = (1 + \beta u)^{-\alpha} \quad (3)$$

Complete analysis of CA-CFAR detector performance is accomplished in [4] when the reference window no longer contains radar returns from a homogeneous background revealing the following detection probability (4) and false alarm probability (5).

$$P_{fa} = [1 + (HC)T]^{-r} [1 + T]^{r-N} \quad (4)$$

where we assumed that the test cell is from clear background.

As the window sweeps over the range cells, more cells from clutter background enter into the reference window. Ultimately, when the cell under investigation comes from a clutter background, we have

$$P_{fa} = M_Z[T/2\mu_0(1+C)] = (1+T)^{-r} (1+T/(1+C))^{r-N} \quad (5)$$

Equations (4) and (5) reduce to the design false alarm rate expression if C is set to zero.

Another situation that may be encountered where the reference window contains nonhomogeneous reference cells is the case of multiple targets. Here, two or more closely spaced Swerling-I targets appear in the reference window. The analysis of the detection probability is similar to the one presented above for the clutter power transitions with some changes in parameters definition. Now P_d is obtained by replacing T with $T/(1+S)$ and C is replaced by I in (5). Thus,

$$P_d = [1 + (1+I)T(1+S)]^{-r} [1 + T/(1+S)]^{r-N} \quad (6)$$

where r now represents the number of interfering targets present in the reference window. Note that the above is a correct expression for the detection probability even though the definitions of C and I assume different noise conditions (thermal noise for C and clutter-plus-thermal noise for I). This is because in the case of clutter power transition the false alarm rate is independent of the thermal noise power μ_0 and in multiple targets the detection probability is independent of the total noise power μ_0 .

The characteristics of the CA-CFAR processor are compared with those of other CFAR processors later in this section. The comparisons demonstrate the superiority of the CA-CFAR processor performance in homogeneous noise background. Nonetheless, its inferior behavior in the nonhomogeneous situation calls for modified CFAR schemes [8].

B. Description of the GO- and SO- CFAR Processors and Performance Comparisons

Excessive numbers of false alarms in the CA-CFAR processor at clutter edges and degradation of detection probability in multiple target environments are the prime motivations for exploring other CFAR schemes that discriminate between interference and the primary targets. Two such techniques have been investigated; both are modifications of the CA-CFAR technique. However, each of these schemes is capable of overcoming only one of the above two problems, with additional loss of detection power. The first scheme that is described in this subsection maintains a constant false alarm rate at clutter edges while the second scheme resolves the primary target in multiple target environments when all the interferers are located in

either the leading or the lagging side of the test cell. A modified detection scheme proposed and analyzed in, known as GO-CFAR procedure, is specifically aimed at reducing the number of excessive false alarms at clutter edges. The total noise power is estimated from the larger of two separate sums computed for the leading and lagging window, as shown in Figure 1(b). For this scheme we have

$$Z = \max(Y_1, Y_2) \quad (7)$$

where

$$Y_1 = \sum_{i=1}^n X_i, \quad Y_2 = \sum_{i=n+1}^N X_i \quad (8)$$

with $n = N/2$. In general, the pdf of Z defined in (7) is given by

$$f_z(z) = f_1(z)F_2(z) + f_2(z)F_1(z) \quad (9)$$

where f_i and F_i are the pdf and cdf, respectively, of the random variable Y_i with Y_1 and Y_2 independent. For a homogeneous background we have $F_i = G(n, 2\mu)$. The false alarm probability in this case is found by computing the mgf of Z it is

$$P_{fa} = 2(1+T)^{-n} - 2 \sum_{i=0}^{n-1} \binom{n+i-1}{i} (2+T)^{-(n+i)} \quad (10)$$

where T is the constant multiplier which depends on the reference window size N and the design P_{fa} . The detection probability P_d is found by simply replacing T with $T/(1+S)$ in (10). The GO modification introduces additional loss of detection compared with the CA-CFAR processor loss when the background is uniform; however, it is found to be less than 0.2dB, which is generally quite acceptable.

The SO-CFAR scheme, on the other hand, has been introduced to alleviate the problems associated with closely spaced targets leading to two or more targets appearing in the reference window. While testing for target presence at a particular range, the processor must not be influenced by the extraneous target echoes. In the SO-CFAR scheme the noise power estimate is the smaller of the sums Y_1 and Y_2 ; as depicted in Figure 1(b). That is,

$$Z = \min(Y_1, Y_2) \quad (11)$$

where Y_1 and Y_2 , are defined in (9). In this case the pdf of Z is given by

$$\begin{aligned} f_z(z) &= f_1(z)[1 - F_2(z)] + f_2(z)[1 - F_1(z)] \\ &= f_1(z) + f_2(z)[F_1(z)F_2(z)f_2(z)F_1(z)] \end{aligned} \quad (12)$$

The expression in the brackets in (12) is simply the pdf of Z for the GO-CFAR scheme given by (9). Therefore, upon substituting (12) into the basic assumption given by [7], the SO-CFAR scheme false alarm probability will be

$$P_{fa} = M_{Y_1}(T/2\mu) + M_{Y_2}(T/2\mu) - P_{fa}^{GO} \quad (13)$$

where $M_{Y_1}(T)$ and $M_{Y_2}(T)$ are the mgfs of Y_1 and Y_2 , respectively and are computed using (12), and P_{fa}^{GO} is the P_{fa} of (10). The expression in (13) gives a very simple relationship between the SO-CFAR processor performance and that of the GO-CFAR processor performance. The detection probability P_d is again given by replacing T with $T/(1+S)$ in (13).

C. Ordered Statistics CFAR Processor

For the OS-CFAR processor, the pdf $f_k(z)$ of random variable x_k is given by

$$f_k(z) = k \binom{N}{k} [1 - F(z)]^{N-k} [F(z)]^{k-1} f(z) = k \binom{N}{k} (1 - e^{-z})^{N-k} e^{-kz} \quad (14)$$

where f is the pdf of square law-detected output for any range cell which is exponentially distributed with pdf

$$f(x) = (1/2\lambda) \exp(-x/2\lambda) \quad (15)$$

and where $\lambda = 1/2$ and F is the corresponding cdf. The detection probability was computed by [4] under the previous assumption as:

$$\begin{aligned} P_d(S) &= k \binom{N}{k} \int_0^\infty x(1 - \exp(-z))^{k-1} \times \text{wpx} \\ &\quad \int_0^\infty (-n - k + 1 + T/(1+S))z dz \\ &= \prod_{i=0}^{k-1} (N-i)/(N-i+T/(1+S)) \end{aligned} \quad (16)$$

Clearly, the constant T is new function of k . The P_{fa} is given by setting $S=0$ in (16). The value of T for a given k is computed by solving iteratively for fixed N and P_{fa} . From previous description of different CFAR schemes we have obtained so far, we may make the following general statements about the performance characteristics of the OS-CFAR processor relative to the mean-level CFAR schemes. Though the OS-CFAR processor exhibits some loss of detection, power in homogeneous noise background compared with the CA and GO processors, reveals superior performance in a multiple target environment [9],[10]. By selecting k to be near the maximum we may attain a false alarm rate performance close to that of the GO-CFAR processor. The OS-CFAR scheme also enjoys many advantages over the SO scheme. The detection performance of the OS-CFAR processor is independent of the location of the interfering targets in the reference window while the SO-CFAR processor suppresses the primary target if the extraneous targets are located in both the leading and the lagging window. Furthermore, the detection performance of the OS-CFAR processor in homogeneous background noise is superior compared to the SO-CFAR processor for k values of interest [11].

IV. SIMULATION RESULTS

Figures 2 and 3 depict the detection probability at various values of false alarm probability and for number of cells $N=8$ and $N=32$, and SNR range from 5dB to 30 dB. At number of cells $N=8$, it is obvious that CA-CFAR scheme achieves maximum detection probability of 0.98 at P_{fa} of 10^{-6} and then uniform degradation occurs at lower values of false alarm probability. In case of GO-CFAR and at the same specifications, detection probability also reaches maximum value of 0.96 at SNR of 30 dB for P_{fa} in the range of 10^{-4} to 10^{-6} P_{fa} , and then degradation happens at lower values of P_{fa} . In the SO-CFAR, detection probability is 0.94 at SNR of 30 dB but severe degradation occurs at lower values of false alarm probability. Also the detection probability in this case approaches zero at lower values of P_{fa} . The CA-CFAR and GO-CFAR reveal acceptable detection probability at SNR > 15 dB. The OS-CFAR processor behaves similar to CA-CFAR but takes longer processing time. The CA-CFAR displays its superiority of detection probability over all other schemes.

Computations takes place at number of cell $N=16$ and $N=32$. The CA-CFAR and GO-CFAR achieve maximum detection probability at P_{fa} of 10^{-6} , and at

$N=16$ the OS-CFAR is like CA-CFAR revealing maximum detection probability at higher values of SNR. When the number of cells becomes 32, the CA-CFAR achieves a detection probability of 0.99 showing superiority in performance, while the GO-CFAR and OS-CFAR respectively, achieve detection probability of 0.98 and 0.97. Clear improvement occurs for the SO-CFAR at SNR of 30 dB, and P_{fa} in the range from 10^{-4} to 10^{-6} .

Hence, the 3D-Matlab in Figures 2 and 3 in addition to the 2D- Matlab in Figure 4 are adequate to differentiate between all CFAR processors but not sufficient to give final decision for the designers of radar CFAR processors about what type of CFAR schemes can be used for known SNR. However, all CFAR schemes are capable to attenuate fixed targets, false targets and interference. Therefore, an emphasizing test will be necessary for all types to ensure which CFAR type is superior in detecting moving targets by simulating an input signal whose horizontal axis is the range cells, and the vertical axis is the amplitude in mV, The

signal contains three moving targets with range cells $n=100, 500$ and 700 as shown in Figure 5.(a), and then in Figure 5(c) after being processed by Doppler filter bank. The case of three fixed targets is depicted in Figure 5.(b) and then in Figure 5.(d) after being processed by Doppler filter bank. The results shown in Figure 6 concern attenuated fixed targets, false targets and interference after being processed by all CFAR schemes. In the case of moving target detection by various CFAR processors, it is obvious in Figure 7.(a)-(e) to Figure 7(e) that the CA-CFAR and GO-CFAR are superior in extracting the three moving targets from noise, interference and false targets. In case of SO-CFAR, the targets appear at their same positions at the range cells $n= 100, 500,$ and 700 . False targets appear for the range cells from 0-80 for both the OS-CFAR and SO-CFAR schemes. To improve the performance of OS-CFAR scheme, many iterations are done to get rid of false targets and interference by increasing the rank of the OS-CFAR scheme as shown in Figure 7.(e)

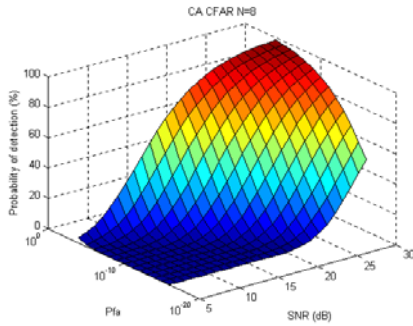


Fig. 2 (a) CA-CFAR processor

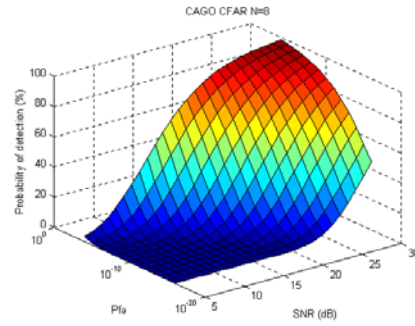


Fig. 2 (c) GO-CFAR processor

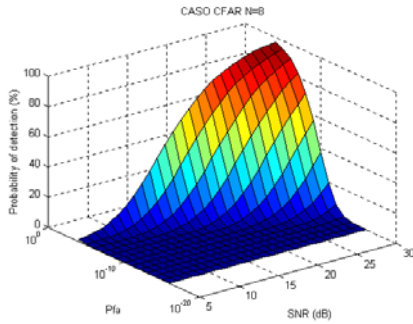


Fig. 2 (b) SO-CFAR processor

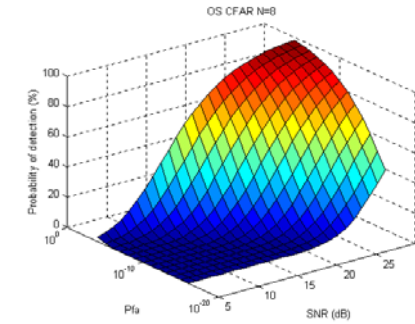


Fig. 2 (d) OS-CFAR processor

Fig. 2 CFAR processor at $N=8$

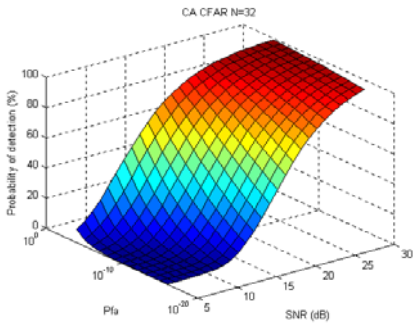


Fig. 3 (a)

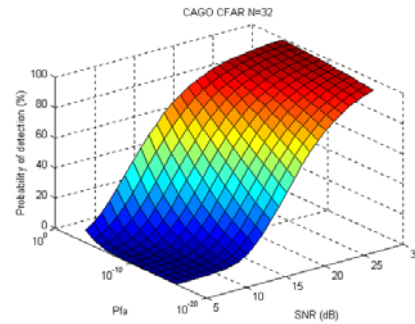


Fig. 3 (b)

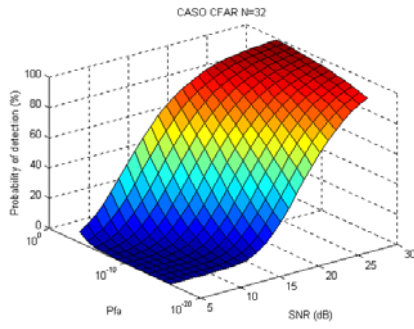


Fig. 3 (c)

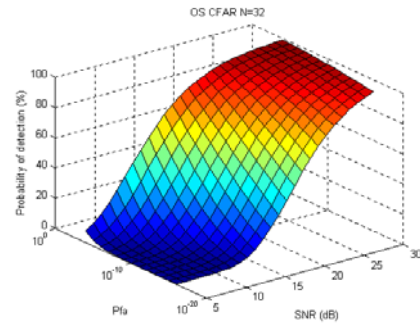


Fig. 3 (d)

Fig. 3 CFAR processor at N=32

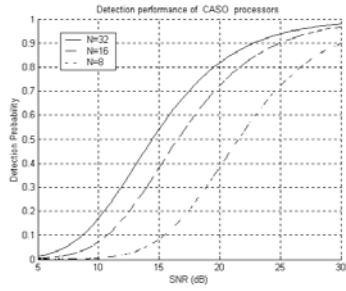


Fig. 4 (a)

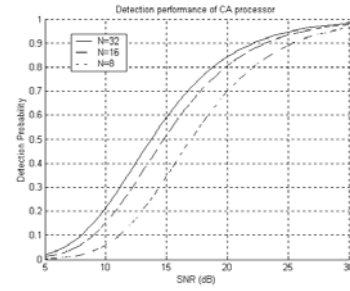


Fig. 4 (b)

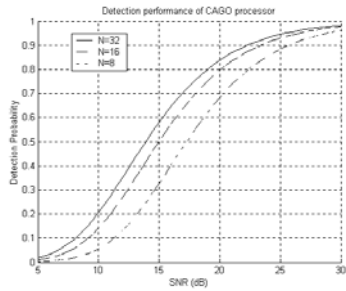


Fig. 4 (c)

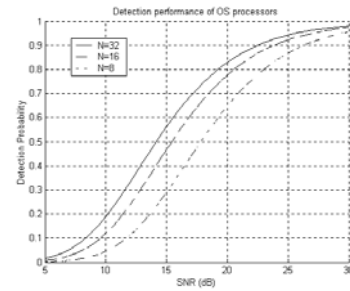


Fig. 4 (d)

Fig. 4 Detection performance of CA-, GO-, SO-, and OS-CFAR processors

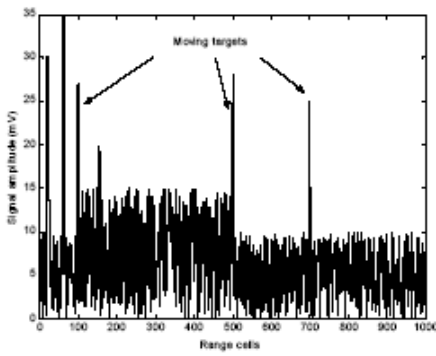


Fig. 5 (a)

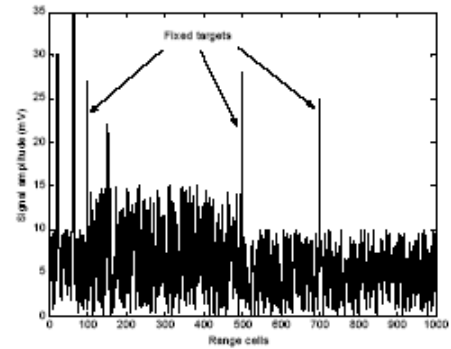


Fig. 5 (b)

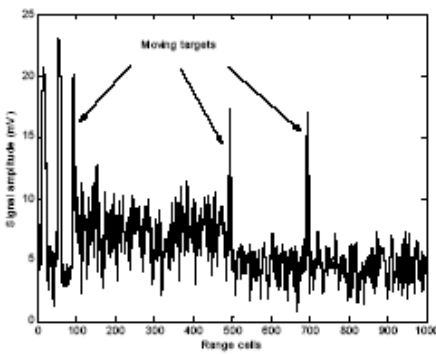


Fig. 5 (c)

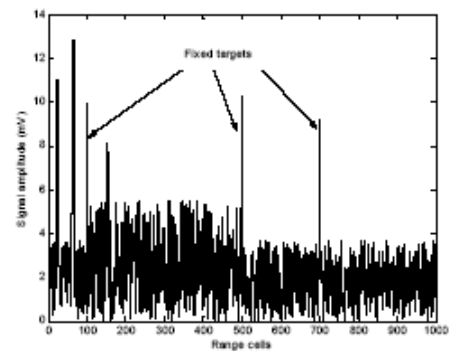


Fig. 5 (d)

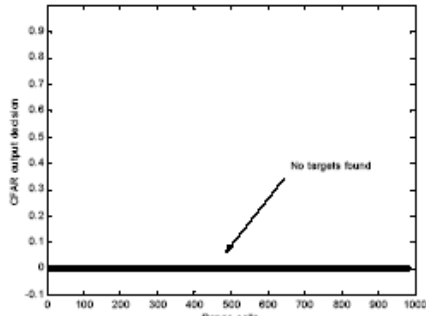


Fig. 6

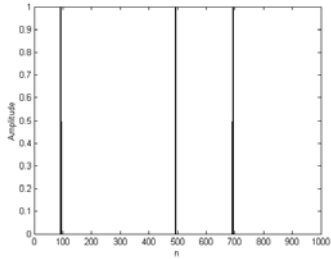


Fig. 7 (b) Signal after (GO-CFAR)

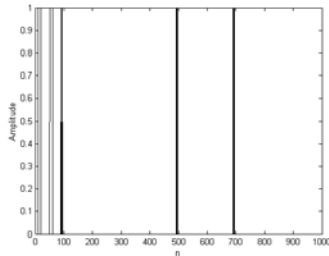


Fig. 7 (d) Signal after (OS-CFAR)

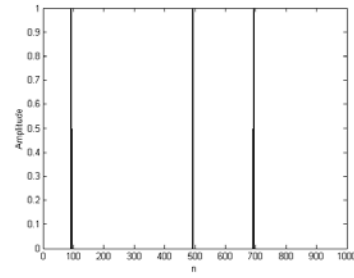


Fig. 7 (a) Signal after (CA-CFAR)

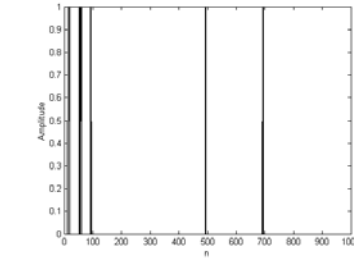


Fig. 7 (c) Signal after (SO-CFAR)

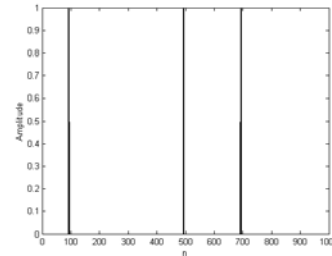


Fig. 7 (e) 10's (OS-CFAR)

V. CONCLUSIONS

The detection performance of the CA-and GO-CFAR processors is superior in case of homogeneous noise background.

For all CFAR processors, the false alarm rate increases considerably at the clutter edges, and multiple targets. Although the false alarm rate of GO processor in regions of clutter transitions is better than that of CA, the detection performance in the multiple target case is poor.

Therefore, the CFAR processors designers must take into account that both the CA-CFAR and GO-CFAR processors enjoy maximum detection probability compared to other processors at various values of false alarm probability.

The SO-CFAR scheme does not appear to offer any advantage over the CA and GO processors. In addition to exhibiting high loss of detection power in homogeneous noise background, the SO-CFAR processor is unable to resolve multiple targets and to control the false alarm rate at clutter edges except when the reference window includes a cluster of radar targets.

It is concluded that the CA-CFAR scheme enjoys the best detection probability among other schemes for both fixed and moving targets, except for high rank OS-CFAR scheme.

REFERENCES

[1] Peebles, *Radar Principles*, McGraw Hill, Book Company, USA, Florida, 1998.
 [2] M. I. Skolnik, *Introduction to Radar Systems*,

McGraw Hill, Book Company, USA, 3rd ed., 2001.

- [3] Rohling, H., "Radar CFAR Thresholding in Clutter and Multiple Target Situations," *IEEE Transactions on Aerospace and Electronic Systems*, vol. 19, pp. 608-621, July 1983.
 [4] Gandhi, P, and Kassam, S.A., "Analysis of CFAR Processors in Non Homogeneous Background," *IEEE Transactions on Aerospace and Electronic Systems*, vol. 24, pp. 427-445, July 1988.
 [5] Simon Haykin, *Adaptive Filter Theory*, Prentice Hall, London, 2002.
 [6] Simon Kingsley, Shaun Quegan, *Understanding Radar Systems*, McGraw Hill, 1992.
 [7] Barton, David, and Leonov, *Radar Technology Encyclopedia*, Norwood, Artech House, 1997.
 [8] Amirmerhararabi, H., and Viswamanathan, R., "A New Distributed Constant False Alarm Rate Detector," *IEEE Transactions on Aerospace and Electronic Systems*, vol. 33, pp. 85-97, Jan. 1997.
 [9] Jian Guan; Ying-Ning Peng; You He; "Proof of CFAR by the Use of the Invariant Test," *IEEE Transactions on Aerospace and Electronic Systems*, vol.:6, pp. 336- 339, Jan. 2000.
 [10] Alaa Hafez, "New Approach to Moving Target Detector (MTD) Implementation in Military Radars," *First Scientific Symposium on Recent Technologies in Electronics & Communications Egypt*, vol. 3, pp.175- 182, Feb. 2003.
 [11] Tri-Tan Van Cao, "A CFAR Thresholding Approach Based on Test Cell Statistics," *IEEE Philadelphia Radar Conference*, vol. 36, pp. 105-111, April 26-29, 2004.